 DOI:10.30420/566414083

Investigation on direct liquid cooling design of power modules with flat baseplate for automotive application

Masahide Kamiya , Nobuhide Arai*1, Shinichiro Adachi*1, Kensuke Matsuzawa*1,
Takahiro Koyama*1,Takanori Shintani*2
*1Fuji Electric Co., Ltd, 4-18-1, Tsukama, Matsumoto, Nagano, Japan
*2Fuji Electric Co., Ltd, 5520, Minami Tamagaki, Suzuka, Mie, Japan

Corresponding author: Masahide Kamiya, kamiya-masahide@fujielectric.com
Topics: 2.3 Thermal Management and Simulations
Preference: Oral Presentation

Abstract

Copper pin fins and aluminum integrated fins have generally been used in power modules for direct liquid cooling. The direct liquid cooling system using copper pin fins or aluminum integrated fins pro-vides excellent heat dissipation, but it is expensive in terms of materials and their production costs. Copper flat baseplates, which are low cost and generally used for indirect liquid cooling or air cooling, have not been adequately evaluated as direct liquid coolers regarding to the cooling performance and reliability in automotive applications. This paper investigates suitable rib shape in direct liquid cooling for a flat baseplate power module from the viewpoints of heat dissipation and pressure loss. In addition, it demonstrates sufficient reliability in terms of coolant corrosion and pressure durability, which are essential for automotive applications.

1Introduction

As electrification of automobiles progress, electrical components such as inverters for motor and generator need to be smaller to increase room space of vehicles. In addition, as conventional gasoline-powered vehicles are replaced with electrified vehicles, it is necessary to reduce the cost of power electronics components. The cost of automotive power modules can be reduced by increasing power density. Fuji Electric has developed direct liquid cooling technology with integrated fin, Reverse-Conducting Insulated Gate Bipolar Transistor (RC-IGBT), and lead frame wiring technology for high power density [1] [2]. Electrification is rapidly expanding not only to SUVs and luxury cars, but also to small and middle power range such as light and compact vehicles, so power range variations in power modules are also required. M682 series, which features a power range of 50-100 kW, have been developed with the concept of a compact package and low cost for the market of light and compact vehicles. The lineup of the M682 series is shown in Fig.1. The package footprint is the same, with a choice of capacity variants depending on the chip size and cooler combination. By using the module, it is possible to standardize peripheral components of the module while changing the capacity range of the inverter, thereby reducing costs, and improving development efficiency through standardization of inverter components. A pin fin cooler is used for the 100 kW output, while a flat baseplate structure is applied to the coolers for the lower outputs of 50 and 75 kW. Flat baseplates have lower heat dissipation performance than copper pin fins. Baseplates have traditionally been used for indirect liquid or air cooling, but direct liquid cooling structures can improve heat dissipation. However, there are few research which the optimum liquid cooling channels for flat bases have been fully investigated for automotive applications. This paper describes the optimum liquid cooling channels for flat bases. In addition, the results of a reliability assessment of the direct liquid-cooled structure for automotive applications are presented. Finally, a comparison of the output performance of modules with flat-based structures in optimized liquid cooling channel is presented.

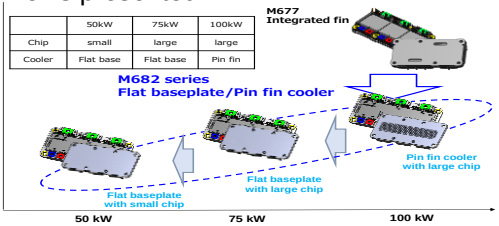

Fig.1 M682 line up

ISBN 978-3-8007-6414-3

 DOI:10.30420/566414083

2 Direct liquid Cooling with a Flat Baseplate

2.1 Thermal resistance of flat baseplate power modules

Flat baseplate coolers are applied in industrial modules and are generally used with an indirect liquid cooling method. In this method, copper base type modules are installed in liquid-cooled heatsinks via grease, which have significantly high thermal resistance. Figure 2 shows the cross-sectional structures of modules and the analysis results of the thermal resistance breakdown. In the direct liquid cooling method, the use of coolers with heat dissipation fins cooled by a coolant circulation system achieves low thermal resistance [3], [4], [5], [6]. With the copper base type in this study, by eliminating grease and adopting a direct liquid cooling approach, a 36% improvement in thermal resistance can be achieved. Furthermore, applying a silicon nitride AMB (Si_3N_4, thermal conductivity 80 W/mK) from an alumina DCB (Al_2O_3,thermal conductivity 20 W/mK) which is widely used as insulated substrates, an additional 12% improvement in thermal resistance can be achieved. As the result, a total improvement of 48% compared to a conventional indirect liquid cooling configuration. The efficiency of heat dissipation performance in direct liquid cooling structures is a key point, thus a study of the flow paths was carried out.

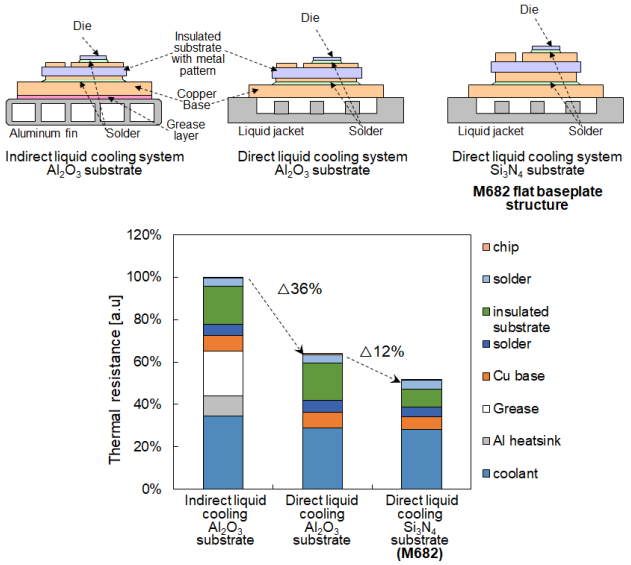

Fig. 2 Comparison of thermal resistance between conventional structure and M682 flat baseplate

2.2 Coolant Flow in Cooling Jacket

The flow of coolant in the liquid cooling jacket was analyzed using Computational Fluid Dynamics (CFD) simulations with a model of a 6 in 1 power module, flowing coolant serially shown in Fig. 3. The simulation condition includes a coolant mixture of long-life coolant and water at a ratio of 1:1, a flow rate of 10 L/min, and a water temperature of 70°C at the inlet. The simulation results of the velocity distribution in the flow channel of the model are shown in Fig. 4. In the flow channel, the coolant tends to flow uniformly, resulting in a uniform distribution of coolant velocity. Cooling of the device generated heat involves transferring heat to the coolant from the surface of the flat baseplate, transporting it for cooling. Therefore, improving the coolant velocity near the surface of the flat baseplate is important for enhancing heat dissipation efficiency. However, increasing coolant velocity leads to increased pressure loss, which must be kept below the allowable pressure loss determined by an electric pump's capacity in automobiles. Hence, low pressure loss is required. Therefore, we investigated models to increase the flow velocity on the back surface of the cooler with lower pressure loss.

Fig.3 Flow Investigation Model (No rib)

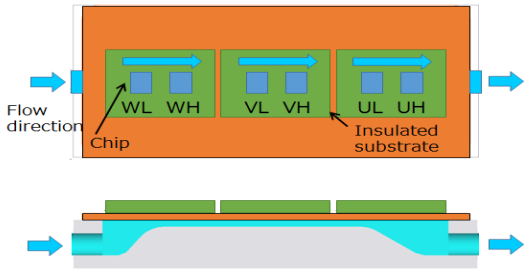

Fig.4 Velocity in liquid cooling jacket (No rib)

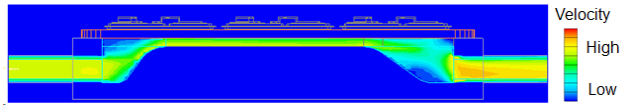

2.3 The Flow Velocity Improvement Effect by Ribs

The rib geometries of the flow channel were studied on simple models that can be machined in the aluminum die-casting process. Figure 5 shows three models with different rib heights and the results of flow analysis in flow rate of 10 L/min and coolant temperature 70°C. Figure 6 shows the analysis of pressure loss and thermal resistance. By adding ribs, it is possible to increase the flow velocity beneath the surface of the flat baseplate. The clearance between the baseplate and the ribs decreases and the flow velocity of coolant increases when high height ribs are applied.

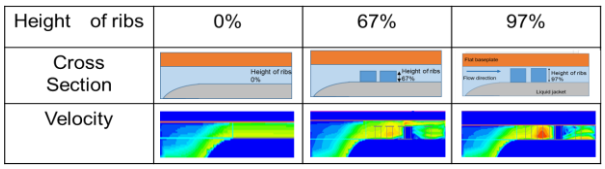

Fig.5 Ribs heights layoutand coolant velocity distribution comparison

 DOI:10.30420/566414083

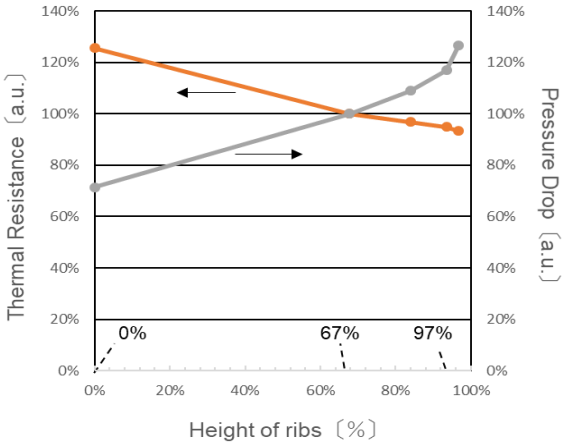

Fig.6 Thermal resistance and pressure loss Dependent on rib heiht in LLC50%,70℃,10L/min

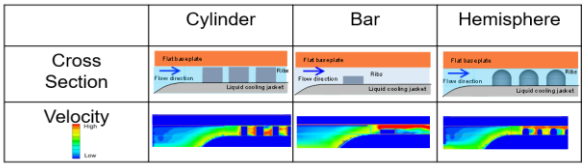

Fig.7 Ribs layoutand coolant velocity distribution comparison

As a result, the thermal resistance decreases .On the other hand, the pressure loss also increases shown in Fig.6. In order to investigate the effects of rib shapes on the pressure loss, simulation was carried out with several rib shapes shown in Fig.7.

The bar structure arranged across the width of the flow channel significantly increases pressure loss. On the other hand, the hemispherical ribs were found to reduce pressure drop while maintaining the same thermal resistance.

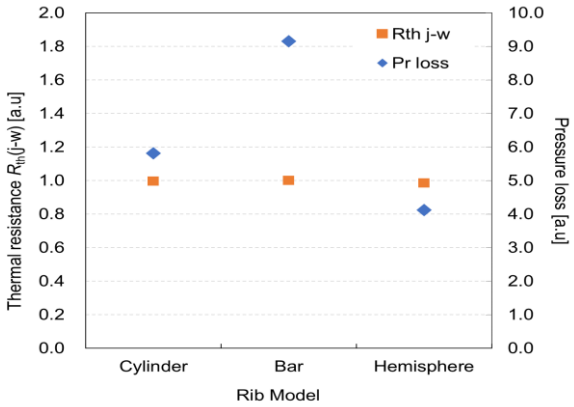

Fig.8.Thermal resistance and pressure loss dependent on rib shape in LLC50%,70℃,10L/min

When the cross-sectional area of the flow channel of the hemisphere is larger than that of the cylinder, the pressure loss of the hemisphere is smaller than the cylinder. Cylinder ribs and hemi sphere ribs are compared with regards to coolant flow. Figure 9 shows schematic diagrams of the cross-sectional structure and the distribution of coolant speed. hemisphere ribs, compared to cylinder ribs, facili-tate the flow of coolant beneath the copper base plate due to the tapered shape of the ribs. In addi-tion, since the coolant collides with the ribs in the direction of flow, it is difficult to flow the coolant in the back of the ribs. However, hemisphere ribs have a smaller effective rib diameter because of tapered shape, reducing the area where the flow is impeded in the back of the ribs. Consequently, hemisphere ribs can enhance flow velocity directly beneath the flat baseplate and promote uniform flow velocity. Analysis of the velocity distribution mapping plot confirms that hemispheres result in more uniform improvement.

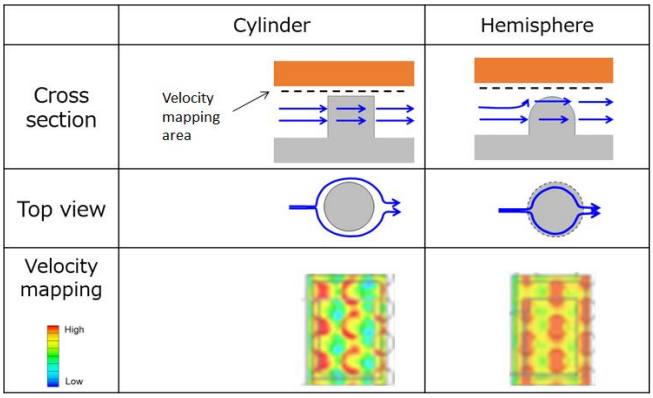

Fig.9 The velocity of coolant distribution between cylinder ribs and hemisphere ribs

2.4 Optimization of Thermal Resistance and Pressure Loss by Rib Arrangement

High-density arrangement of ribs significantly increases pressure loss. Therefore, a study was conducted to reduce pressure loss by adjusting the number of ribs. In addition, experimental verification was carried out to validate the analysis.

Experiments were conducted by making liquid cooling channel parts using a resin 3D printer, varying the density of the ribs, and investigating cooling performance.

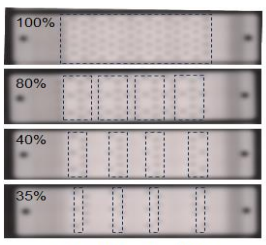

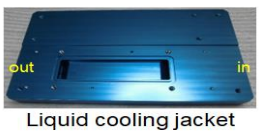

Fig. 10 Evaluation liquid cooling jacket and 3D printed pattern

 DOI:10.30420/566414083

The evaluation liquid cooling jacket is made of aluminium and features several patterns of plastic coolant channel models for performance comparison. The testing environment involves a coolant circulation with LLC 50%, 70°C, and a flow rate of 10 L/min. The junction temperature of the chips was measured using on-chip sensor diodes. Pressure losses were measured at the inlet and outlet of the liquid jacket using a differential pressure measurement system. Figure 8 shows the impact of rib spacing on thermal resistance along with sample evaluations.

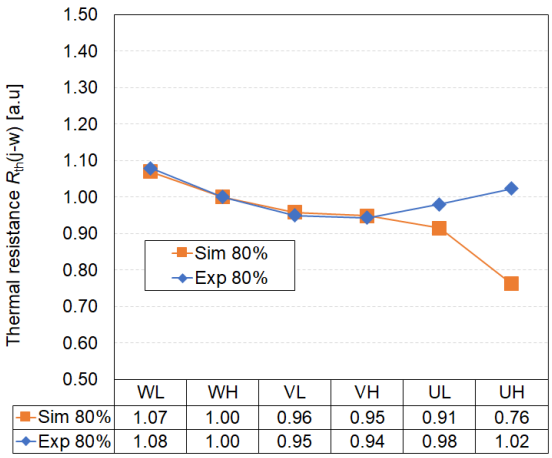

	WL	WH	VL	VH	UL	UH
Sim 80%	1.07	1.00	0.96	0.95	0.91	0.76
Exp 80%	1.08	1.00	0.95	0.94	0.98	1.02

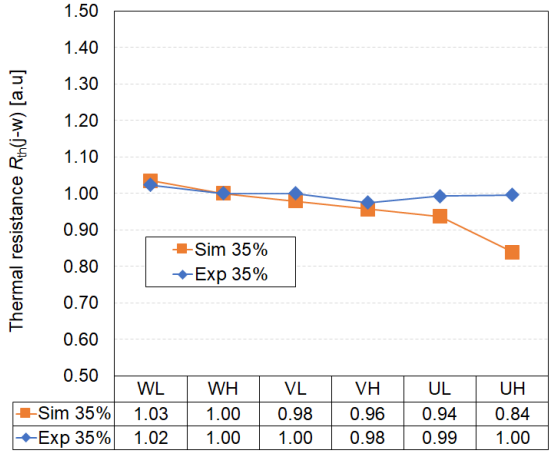

	WL	WH	VL	VH	UL	UH
Sim 35%	1.03	1.00	0.98	0.96	0.94	0.84
Exp 35%	1.02	1.00	1.00	0.98	0.99	1.00

Fig.11 Simulation and experiment results

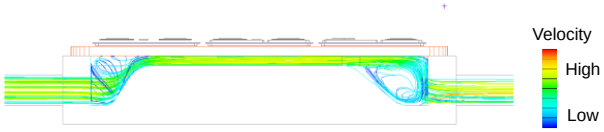

Fig. 12 The coolant flow in hemisphere ribs

It can be found that the thermal resistance distribution is in good agreement between experiment and simulation, except for 1 arm (UH). The difference of thermal resistance UH could be caused by the generation of vortices causing discrepancies between experiment and simulation shown in Fig. 13. Countermeasures can be implemented in the outlet side flow path geometry to mitigate this effect. Since the thermal resistances of the chips placed in the middle of the 6 in 1 module such as WH, VL and VH have a good agreement between experiment and simulation, the relationship between thermal resistances, pressure losses, and the spacing ratio is analysed in VH shown in Fig. 10.

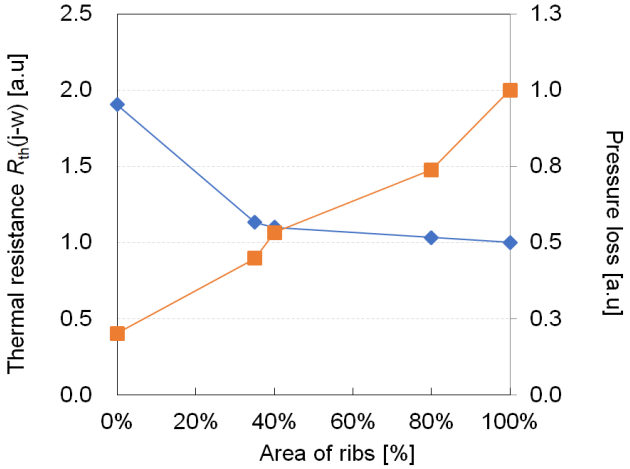

Fig. 13 Area of ribs dependence of thermal resistance and pressure loss

Analysing the coolant velocity obtained through simulation, the relationship between velocity and spacing ratio is shown in Fig. 14 Plotting velocity against thermal resistance reveals that thermal resistance decreases gradually as the spacing ratio decreases from 100% but exhibits a sharp decline at 35%.

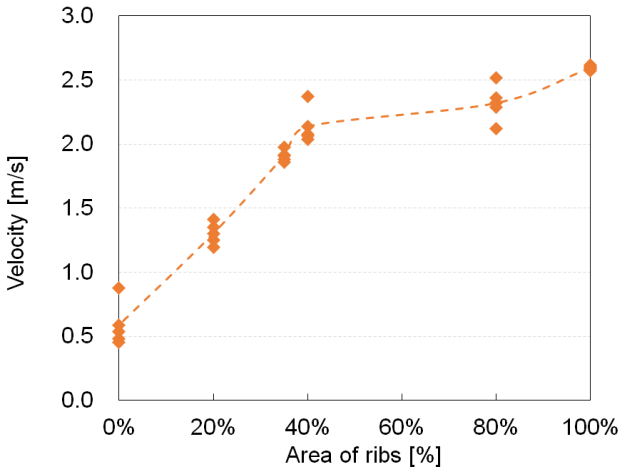

Fig. 14 Area of ribs dependence of the velocity of coolant

From these results, it is found that

- The thermal resistance and the pressure loss in direct liquid cooling with a flat baseplate are dependent on the flow velocity likewise fin structures. Flow velocity is influenced by the spacing ratio of the ribs, with a sharp decrease

ISBN 978-3-8007-6414-3

 DOI:10.30420/566414083

observed beyond a certain point, around 35%. This is because when the proportion of ribs in the flow channel cross-section is too low, the coolant does not flow directly beneath the base.

- By maintaining a spacing ratio of 40% or higher, where the flow velocity does not decrease significantly, it is possible to adjust thermal resistance and pressure distribution effectively by ensuring an appropriate proportion of ribs.

3 Reliability Test

3.1 Corrosion Test

In the performance validation of thermal resistance and pressure loss, evaluations were carried out using 3D printed plastic channel models for the sake of simplicity. However, in actual inverter housings, the liquid cooling channel is often formed together with ADC12 aluminum material through aluminum die-casting process. On the other hand, flat baseplate coolers are made of copper and are surface covered with nickel plating to prevent copper corrosion. However, under the worst-case scenario of rib tolerances, there is a possibility of the contact between the flat baseplate and the aluminum housing ribs of the flow channels. Concerns arise about corrosion due to the potential difference between the nickel plating and aluminum, which could lead to corrosion of the nickel plating and exposure of copper. This could accelerate copper corrosion and deteriorate thermal performance.

The evaluation of corrosion resistance using a corrosive liquid was conducted. The corrosion test was performed using a copper flat baseplate with Ni plating and an ADC12 inverter housing. As the corrosive liquid, OY water is applied. OY water is formulated to be even more corrosive than the most corrosive water found through global water quality survey [7]. The solutions of OY water and long-life coolant mixed in a 1:1 ratio is used. Table 1 shows the conditions for the corrosion test and Fig. 15 presents a schematic diagram of the sample and the test setup. The inverter test work which initially contact with the baseplate was prepared. An evaluation was conducted.

Table 1. Corrosion test condition

Corrosion test		
Test water	OY water : LLC 50% = 1: 1	
OY water	CL^-	195 ppm
	SO_4^{2-}	60 ppm
	Cu^{2+}	1 ppm
	Fe^{3+}	30 ppm
LLC 50%	Long Life Coolant 50 %	
Temperature	65 ℃	
Flow rate	12 L/min	
Test time	1000 hr	

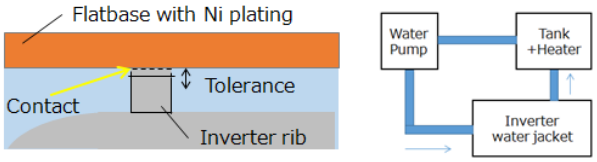

Fig. 15 Cross-section of sample and test set up

Figure 16 shows the test results and analysis findings. Although there is some discoloration, no pitting corrosion was observed on the nickel plating of the cooler. Additionally, there was no discoloration or pitting corrosion observed on the liquid cooling jacket rib side. Surface analysis of the plating was conducted using Energy Dispersive X-ray Spectroscopy (EDX) for elemental analysis. EDX analysis at red circle area contact with the water revealed the presence of carbon (C) and oxygen (O), which are the main components of long-life coolant, and sulfur (S) and chlorine (Cl), elements of the corrosive fluid. It was confirmed that the plating remained intact without exposing copper. Fig. 17 describes the thermal resistance evaluation results at initial, 500 hours, and 1000 hours. There was no increase in thermal resistance on the cooler side after a 1000-hour corrosion test. Based on these results, it was confirmed that the cooler exhibited corrosion resistance in the corrosion cycling test.

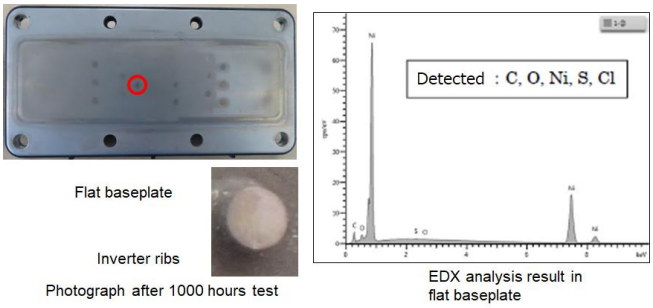

Fig. 16 Sample surface and EDX analysis result after the corrosion test

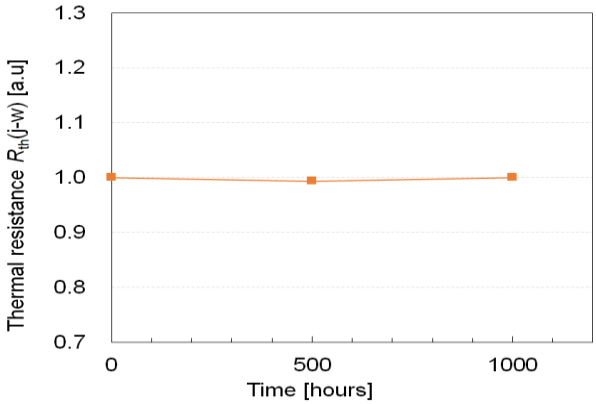

Fig. 17 Evaluation results of thermal resistance during the corrosion test

 DOI:10.30420/566414083

3.2 Intermittent Pressure Test

When an inverter system including a cooling system is started in vehicles, an electric pump starts to work, and high pressure applies to power modules from the cooling system. The seal of a cooling circuit is maintained by O-rings installed between an inverter housing and a power module, but inadequate Moreover, the degradation of the solder layer on a flat baseplate can be considered due to deformation of the flat baseplate.

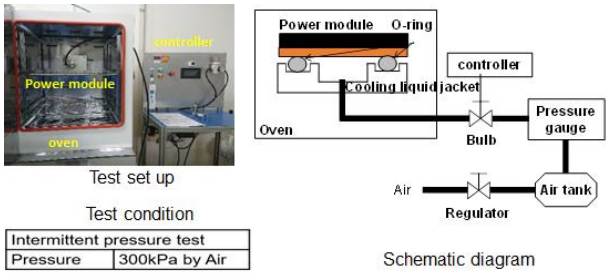

Test condition

Intermittent pressure test	
Pressure	300kPa by Air

Fig. 18 Intermittent pressure test setup and condition

Therefore, an intermittent pressure test was conducted to verify the reliability of the sealing system under the pressure condition shown in Fig14. The test was carried out pressurizing the power module and fixture with air at 300 kPa. The results showed no increase in the thermal resistance in Fig.19. Moreover, ultrasonic inspection confirmed no solder cracks beneath the insulating substrate in Fig.20. Therefore, it was confirmed that the power module has the required pressure resistance for automotive applications.

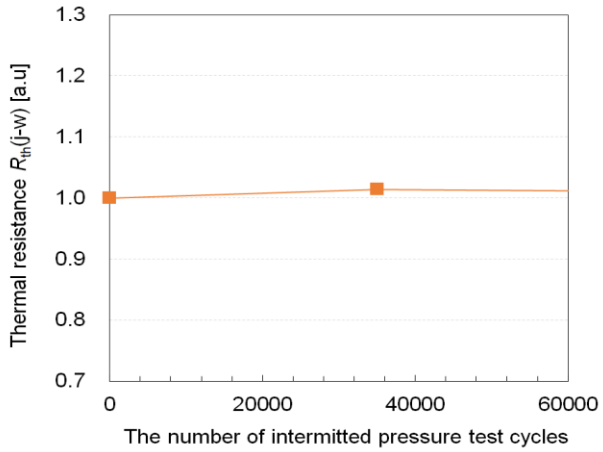

Fig. 19 Evaluation result in thermal resistance during the intermitted pressure test

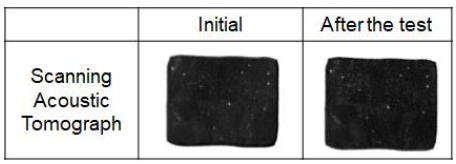

Fig. 20 Scanning acoustic tomograph of the solder layer under the insulated substrate

4 Output Power of M682 with a flat baseplate

The output current of the new power module M682 75 kW using a flat baseplate and silicon nitride insulating substrate was calculated compared with a conventional configuration power module having the same electrical performance of M682 75 kW with indirect liquid cooling and alumina insulating substrate. Figure 18 shows the junction temperature calculation results. It is found that the M682 75kW can achieve 1.5 times the output current compared to the conventional configuration power module.

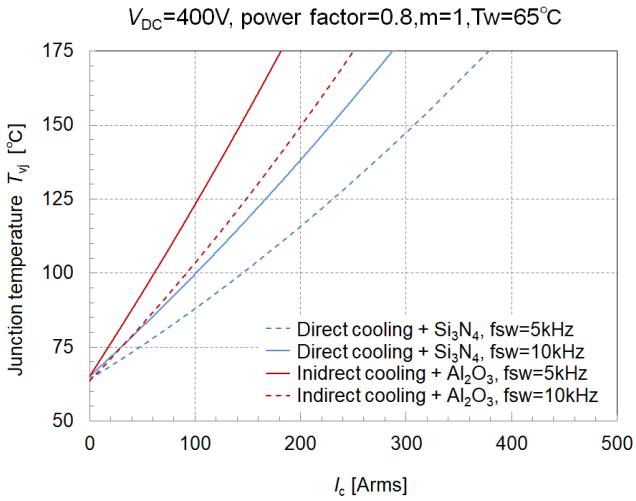

Fig. 21 Junction temperature calculation results

5 Conclusion

In this paper, effective ribs shapes that improves the cooling performance and pressure loss are discussed. Hemisphere rib structure is suitable for coolant flow beneath the flat baseplate and lower pressure loss. Moreover, it was clarified that the design of the cooler can adjust both thermal resistance and pressure loss by adjusting the arrangement of cooling channel ribs. Finally, the cooling system's reliability was confirmed through coolant corrosion test and intermittent pressure tests suitable for automotive applications. Finally, by using the optimal rib shape, the output performance can be improved by 50% percentage compared to the conventional indirect liquid-cooled configuration.

References

[1] S. Adachi, T. Obata, N. Arai, N. Higashi, Y. Tateishi, “Ultra-Compact Automotive Power Module for 100 kW xEV Application”, PCIM Europe 2022, pp.1035-1038.

[2] Y. Sato, S. Adachi, H. Gohara, N. Higashi, S. Yoshida, “Advantage of Lead-Frame Wiring and High Reliable to Electromigration Package for

High Power Density Automotive Power Module", PCIM Europe 2023, pp. 1674-1679.

[3] S. Adachi, F. Nagaune, H. Gohara, T. Hitachi, A. Morozumi, P. Dietrich, A. Nishiura, "High thermal conductivity technology to realize high power density IGBT modules for electric and hybrid vehicles, PCIM Europe 2012, pp.1378-1384.

[4] H. Gohara,Y. Nishimura, A. Morozumi, P. Die trich, E. Mochizuki, Y. Takahashi, "Next-gen IGBT module structure for hybrid vehicle with high cooling performance and high temperature operation", PCIM Europe 2014, pp. 1187-1194.

[5] K. Higuchi, T. Koyama, A. Kitamura, S. Soyano, Y. Takamiya, H. Gohara, S. Yoshida, H. Kobayashi, Y. Nishimura, T. Heinzel, A. Nishiura, "New standard 800A/750V IGBT module technology for automotive application", PCIM Europe 2015, pp.1137-1144.

[6] Y. Tamai, S. Ewald, R. Kato, K. Yamauchi, H. Gohara, T. Yamazaki, "Fourth Generation Aluminum Direct Water Cooling Structure with High Reliability for Automotive Electric System", PCIM Asia 2020, pp.207-210.

[7] H. Tanaka, H. Ikeda, "Influence of Fe and Ni addition on corrosion resistance of aluminum alloy-clad sheet for automotive radiators in weakly alkaline LLC solution", Journal of The Japan Institute of Light Metals, Vol. 70, No. 10, 2020, pp. 451-458.

